RSC Medicinal Chemistry

ROYAL SOCIETY OF CHEMISTRY

RESEARCH ARTICLE

View Article Online
View Journal | View Issue

Cite this: *RSC Med. Chem.*, 2025, **16**, 2808

Indolylmaleimide derivatives as a new class of anti-leishmanial agents: synthesis and biological evaluation†

Samarpita Das, [a] Neerupudi Kishore Babu,[b] Priyanka Mazire,[c] Amit Roy,[c] Rohit Kumar, [a] Sushma Singh[b] and Deepak K. Sharma *[a]

Received 11th February 2025,
Accepted 9th March 2025

DOI: 10.1039/d5md00132c

rsc.li/medchem

Leishmaniasis is a neglected tropical disease, primarily affecting poor and developing countries. The present therapeutic approach faces various limitations, such as concerns regarding toxicity, route of administration, and the emergence of drug resistance. Therefore, there is a critical need to identify novel scaffolds to combat this fatal parasitic infection. Leishmanial DNA topoisomerase 1B is a heterodimeric protein and plays a crucial role in resolving topological problems during various biological processes. It is structurally distinct from its human counterparts, making it an attractive target for drug discovery. In this study, we synthesized various aminated indolylmaleimide derivatives targeting the leishmanial topoisomerase 1B enzyme. *In vitro* leishmanicidal assays on *Leishmania promastigotes* identified one highly potent hit (**3m**), showing considerable inhibition with single-digit micromolar IC_{50} values. Moreover, molecular docking analysis of the potent hit (**3m**) confirmed its strong binding affinity with the enzyme. Thus, the hit molecule (**3m**) holds promise as a lead for developing novel therapeutic strategies against leishmaniasis.

1. Introduction

Leishmaniasis is a vector-borne infectious disease of global importance, affecting a large population in tropical and subtropical regions. This neglected disease is chronic in geographically distinct areas of Asia, Europe, the Middle East, Northern Africa, southeastern Mexico, and other parts of South America.[1,2] The causative agent of the disease is a unicellular protozoan parasite of the genus *Leishmania*, belonging to the family *Trypanosomatidae* and order *Kinetoplastida*. These unicellular protists exist in two different forms, exhibiting a digenetic life cycle. The promastigote form, which resides extracellularly in the gut of sandflies, is flagellated, whereas the amastigote form, found in host macrophages, is non-flagellated.[3] Present chemotherapy for leishmaniasis heavily relies on first-line drugs, including pentavalent antimonials, followed by amphotericin B, miltefosine, and paromomycin as second-line drugs of choice.[4,5] These parenteral drugs are quite unsatisfactory due to numerous limitations, including toxic side effects, prolonged treatment duration, emergence of drug resistance, and exorbitant costs.[6] Due to these drawbacks, none of the available anti-leishmanial drugs can be considered ideal for eliminating parasites from all infected individuals. Therefore, the development of new scaffolds with novel molecular targets and intervention strategies, accompanied by improved safety profiles, remains highly desirable.

Amongst the various anti-leishmanial scaffolds reported, indole alkaloids have shown promising pharmacological activity against the *Leishmania* parasite. In a recent study, we demonstrated that the 3,3′-diindolylmethane (DIM) scaffold stabilizes the topoisomerase 1-DNA complex by arresting DNA relaxation activity, ultimately inhibiting replication and transcription processes, which leads to apoptotic cell death in the parasites.[7,8] The most active compound in our DIM series (**A**) showed an IC_{50} value of ~31 μM against *L. donovani* promastigotes (Fig. 1). To improve anti-leishmanial activity and topoisomerase 1 inhibition, we extended our investigation to the indolylmaleimide scaffold. The indolylmaleimide moiety is found in several biologically active natural products (granulatimide, arcyriaflavins, staurosporine, rebeccamycin, and aqabamycin G) and is well-documented for its anti-tumor activity through the inhibition of protein kinases and topoisomerases.[9–11] It has been reported that indolylmaleimide-based compounds with a

[a] *Department of Pharmaceutical Engineering and Technology, Indian Institute of Technology, Banaras Hindu University, Varanasi-221005, India. E-mail: deepak.phe@itbhu.ac.in*
[b] *Department of Biotechnology, National Institute of Pharmaceutical Education and Research (NIPER), Sector-67, S.A.S., Nagar (Mohali)-160062, India*
[c] *Department of Biotechnology, Savitribai Phule Pune University, Pune-411007, India*

† Electronic supplementary information (ESI) available: The experimental protocols, molecular characterization data and NMR spectra (^{1}H, ^{13}C, and ^{19}F) of all the compounds are provided in the supporting information file. See DOI: https://doi.org/10.1039/d5md00132c

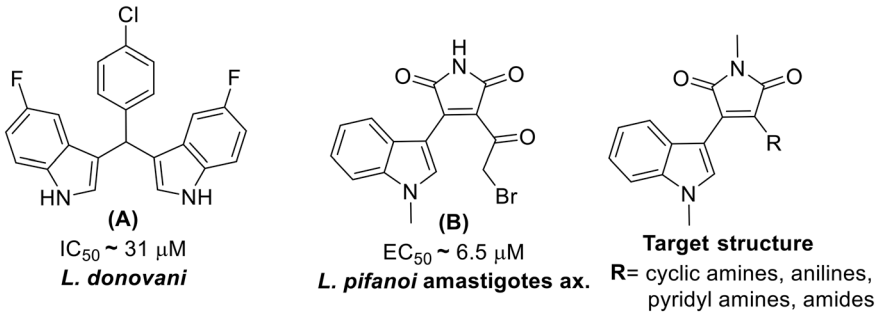

Fig. 1 Literature reported 3,3′-DIM (**A**) and indolylmaleimide (**B**) are active against the *Leishmania* parasite. Target structure for anti-leishmanial activity in the present study.

methyl group on the imide nitrogen result in the loss of PKC inhibition and exhibit anti-tumor activity *via* inhibition of topoisomerase 1. Recently, Gil and co-workers[12] screened the LeishBox collection of leishmanicidal compounds developed by GlaxoSmithKline and identified compound **B** (Fig. 1), which contains the indolylmaleimide scaffold. This compound showed activity against *L. pifanoi* axenic amastigotes, with an EC_{50} value of ~6.5 Mm, and was devoid of cytotoxicity in HepG2 and THP-1 cells. Overall, these literature reports prompted us to explore the effect of indolylmaleimide with a methyl group on the imide nitrogen towards inhibiting leishmanial topoisomerase 1 for anti-leishmanial activity.

In this study, we synthesized 3-amino-4-indolylmaleimides and 3-amido-4-indolylmaleimides from a common precursor using nucleophilic substitution and the Buchwald–Hartwig cross-coupling reaction (target structure, Fig. 1). Our current work focuses on the inhibition of leishmanial topoisomerase 1B using aminated indolylmaleimide derivatives to prevent the growth and proliferation of *L. donovani* parasites. Two series of these hybrid indolylmaleimide molecules have been carefully designed and synthesized by a simple nucleophilic substitution with aliphatic and heterocyclic amines as well as coupled with aromatic anilines and aminopyridines *via* the Buchwald–Hartwig cross-coupling reaction. Our preliminary studies with the 44 molecules revealed that one molecule (**3m**) was the most active with an IC_{50} of ~4 μM. Mechanistic studies with **3m** suggest that it causes significant cellular damage. Computational predictions and enzyme inhibition assays confirm that **3m** inhibits leishmanial topoisomerase 1B, leading to parasitic cell death.

2. Results and discussion

2.1 Synthesis of indolylmaleimide derivatives and their leishmanicidal activity analysis

We synthesized 3-amino-4-indolylmaleimides (**3a**–**3n**), 3-anilino- and 3-pyrido-4-indolylmaleimides (**4a**–**4r**), and

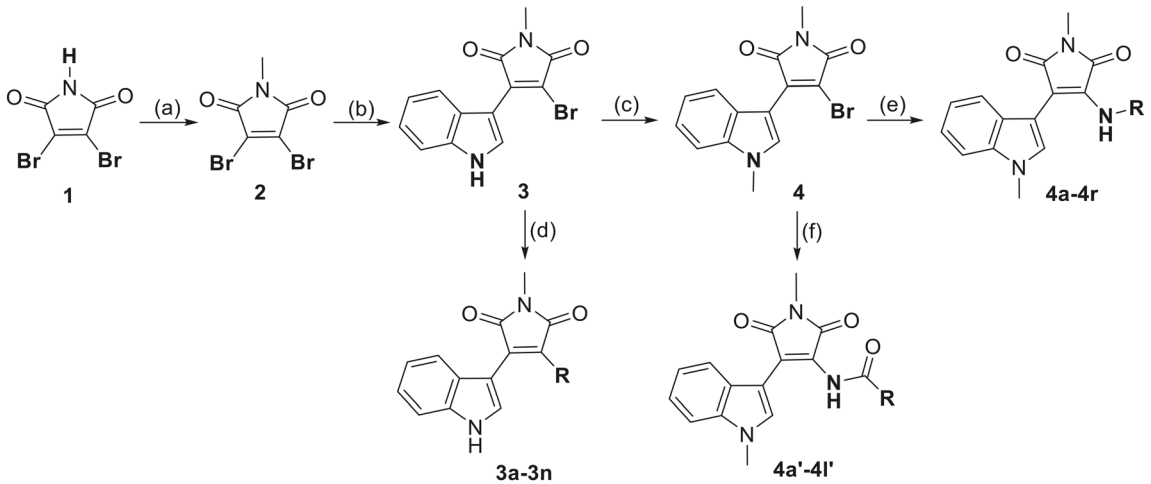

Scheme 1 The synthetic routes of target compounds **3a**–**3n**, **4a**–**4r**, and **4a′**–**4l′**.[a] [a]Reagents and conditions: (a) **1** (4 mmol), iodomethane (1.2 eq.), K_2CO_3 (1.5 eq.), acetone, rt, 2 h, 92%;[b] (b) **2** (3.7 mmol), indole (2 eq.), EtMgBr (2.05 eq.), dried THF, rt, 2 h, 65%;[b] (c) **3** (1 mmol), iodomethane (1.2 mmol), K_2CO_3 (1.5 mmol), acetone, rt, 2 h, 72%;[b] (d) **3** (0.2 mmol), Et_3N (2 eq.), amines (1.2 eq.), DMF, heat at 100 °C for 16 h, 23–92%;[b] (e) **4** (0.5 mmol), anilines or aminopyridines (1.5 eq.), Cs_2CO_3 (1.5 eq.), $Pd_2(dba)_3$ (5 mol%), xantphos (10 mol%), toluene (3 mL), 100 °C, N_2 atmosphere for 12 h, 52–88%;[b] (f) **4** (0.3 mmol), aliphatic or aromatic amides (1.5 eq.), Cs_2CO_3 (1.5 eq.), Cs_2CO_3 (1.5 eq.), $Pd_2(dba)_3$ (5 mol%), xantphos (10 mol%), toluene (3 mL), 100 °C, N_2 atmosphere for 12 h, 57%–85%.[b] [b]Isolated yields.

3-amido-4-indolylmaleimides (**4a′–4l′**) using the synthetic routes depicted in Scheme 1. Commercially available 3,4-dibromo-1*H*-pyrrole-2,5-dione (**1**) was converted into its *N*-methyl analog (**2**) by simple methylation using iodomethane in the presence of a base. Furthermore, coupling of 1*H*-indole with **2** was carefully conducted in the presence of Grignard reagent using a reported method to produce the main precursor 3-bromo-1-methyl-4-(1-methyl-3-indolyl)maleimide (**3**).[13] *N*-Methylation of intermediate **3** gave the precursor **4**. *N*-protection of indole in **4** was necessary to prevent interference in subsequent coupling reaction steps. Nucleophilic substitution of the bromine atom of **3** with various primary and secondary amines at elevated temperature afforded target compounds, 3-amino-4-indolylmaleimides (**3a–3n**). Subsequent treatment of intermediate **4** with an array of anilines and 2-aminopyridines, catalyzed by $Pd_2(dba)_3$/xantphos using Buchwald–Hartwig coupling yielded the target 3-anilino- and 3-pyrido-4-indolylmaleimides derivatives (**4a–4r**).[14,15] Compound **4** was also subjected to Buchwald–Hartwig coupling with several aliphatic and aromatic amides to afford the target 3-amido-4-indolylmaleimides derivatives (**4a′–4l′**).[14] Among the 44 synthesized derivatives, **3m** and **3n** were the most potent with IC_{50} values of 6.6 ± 1.15 μM and 24.56 ± 1.89 μM, respectively (Table 1). Twenty-three derivatives were moderately active with IC_{50} values between 29 to 50 μM and the remaining 19 derivatives were weakly active with IC_{50} > 50 μM. Amphotericin B was used as the standard drug in experiments, displaying an IC_{50} value of 0.42 ± 0.05 μM, consistent with previous studies.[16,17]

2.2 Structure–activity relationship (SAR) analysis

Next, we established a SAR of the synthesized analogues **3a–3n**, **4a–4r**, and **4a′–4l′** corresponding to their anti-leishmanial activity based on the obtained IC_{50} values (Table 1). Simple substitution of 1-methyl-4-indolylmaleimide with five to six-membered heterocyclic amine rings, such as pyrrole, piperidine, morpholine, thiomorpholine, and *N*-methyl piperazine gave rise to derivatives **3a–3e** that exhibited IC_{50} values between 29–34 μM. Expansion of the ring size from **3a** to **3b** does not result in a significant change in the activity. However, the presence of another heteroatom in the ring system leads to a minute improvement of activity as shown in **3c–3e**. Replacement of the *N*-methyl group of the piperazine ring with benzyl or substituted aryl groups (compounds **3f–3h**) moderately decreased the anti-leishmanial activity. Next, we aimed to explore the effect of alicyclic amines on the compound activity; there was a decreasing trend in the IC_{50} values with an expansion of the hydrophobic alkyl ring (**3j–3l**). Direct attachment of smaller alkyl chains functionalized with an electron-withdrawing group such as a trifluoroethyl (CF_3CH_2–) led to an active compound with an IC_{50} value of 6.6 μM: **3m**. Direct substitution with benzylamine led to the formation of another moderately active compound with an IC_{50} value of 24.56 μM (**3n**). **4a–4r** were synthesized from various anilines and aminopyridines adorned with electron-donating and electron-withdrawing groups and the replacement of the small chain alkyl amine with a bulky hydrophobic aryl amine led to a steady decline in the anti-leishmanial activity of the compounds. Among **4a–4r**, compounds containing electron-donating substitutions (–CH_3, –OCH_3, and 2,6-CH_3) at the *para* position of aniline (**4b–4d**) exhibited a complete loss of activity. A similar observation was made in derivatives with electron-withdrawing groups, such as –NO_2, –Br, –Cl, *etc.*, as shown in **4g–4j**, and also in disubstituted anilino derivatives (**4k–4o**), except for **4n** which shows moderate potency with an IC_{50} value of 26.5 μM. **4e**, **4f**, and **4i** containing –CF_3, –OCF_3, and –F groups showed IC_{50} values between 47–49 μM. The replacement of aniline with aminopyridine did not produce the desired effect in **4p** and **4q** but a –CF_3 group in **4r** leads to an IC_{50} value of ~48 μM. When anilines were replaced with various aliphatic and aromatic amides in **4a′–4l′**, the activity trend was altered substantially. Alkyl amido derivatives (**4a′–4d′**) showed a gradually decreasing trend of activity with increasing chain length, with the *tert*-butyl substituted analogue (**4d′**) having the most effectivity with an IC_{50} value of ~30.14 μM. Replacement of the alkyl chain with an alicyclic ring elevates the IC_{50} of the resultant compounds (**4e′** and **4f′**) leading to poor anti-leishmanial activity. **4g′–4l′** containing aryl amide substitution also showed poor leishmanicidal activities. Thus, we can infer that small alkyl amino chains are better tolerated than aryl or alicyclic amine derivatives from the SAR. The presence of fluorine atoms is crucial for leishmanicidal activity. The anti-leishmanial activities of fluorine-containing compounds could be due to the formation of favorable halogen bonds with the binding residues of the active site of the *L. donovani* topoisomerase 1B.

2.3 Anti-amastigote activity and specificity index analysis

Two distinct morphological forms constitute the digenetic life cycle in the *Leishmania* parasite: the motile promastigote form and the non-motile amastigote form. In particular, the amastigotes (virulent form) are prevalent in the parasitophorous vacuoles of macrophages and are formed during diseased conditions.[18,19] Consequently, it is fundamental to assess the effect of potent hits on amastigote growth inhibition and control proliferation inside macrophages for the determination of potential drug candidates. In the present study, *L. donovani*-infected RAW 264.7 cells exposed with the most potent molecule (**3m**) at variable concentrations (2.5 μM, 5 μM, 7.5 μM, and 10 μM) revealed a dose-dependent decrease in intracellular macrophage infection with respect to the infected control. In the untreated control, ~85% of macrophages were infected, while only 10–50% infection was observed in the presence of different concentrations of **3m** (Fig. 2A). Next, the number of amastigotes per 100 macrophages was counted microscopically to determine the intracellular amastigote

Table 1 Indolylmaleimide (IM)-based derivatives from Scheme 1 and their potency against *L. donovani* promastigotes

Compound	R=	Yield (%)	IC_{50} (μM)
3a		82	33.04 ± 1.45
3b		75	34.42 ± 1.24
3c		72	29.22 ± 1.97
3d		80	29.03 ± 1.83
3e		76	32.92 ± 1.65
3f	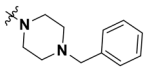	92	38.04 ± 2.92
3g	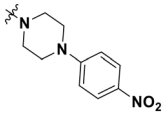	77	36.09 ± 1.54
3h	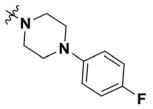	78	38.22 ± 2.78
3i	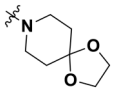	85	34.02 ± 2.09
3j		54	33.91 ± 1.81
3k	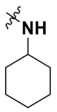	23	37.45 ± 1.56
3l	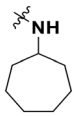	49	41.95 ± 2.96
3m	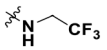	65	**6.6 ± 1.15**
3n	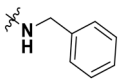	47	**24.56 ± 1.89**
4a		88	>50
4b	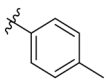	85	>50
4c	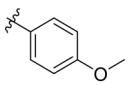	82	>50
4d		83	>50
4e	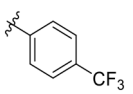	72	49.34 ± 2.98

Table 1 *(continued)*

Compound	R=	Yield (%)	IC_{50} (μM)
4f	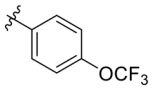	75	47.26 ± 2.38
4g	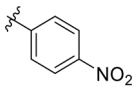	76	>50
4h	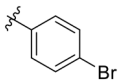	78	>50
4i	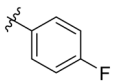	65	48.07 ± 2.56
4j	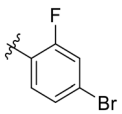	54	>50
4k	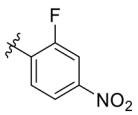	69	>50
4l	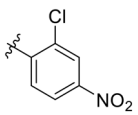	66	>50
4m	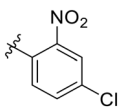	54	>50
4n	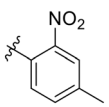	57	**26.5 ± 3.5**
4o	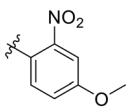	52	>50
4p		59	>50
4q	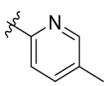	55	>50
4r	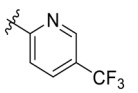	52	48.33 ± 2.67
4a′	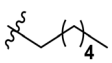	85	31.26 ± 1.67
4b′	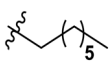	82	32.09 ± 1.63
4c′	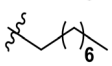	79	32.32 ± 1.28
4d′		64	30.14 ± 1.56
4e′		57	41.10 ± 2.87
4f′		61	45.09 ± 2.93

Table 1 *(continued)*

Compound	R=	Yield (%)	IC_{50} (μM)
4g′	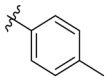	78	>50
4h′	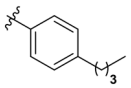	81	>50
4i′	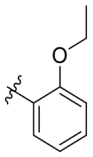	72	>50
4j′	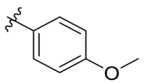	67	>50
4k′	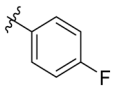	65	48.03 ± 2.89
4l′		56	>50
Amphotericin B (standard)	—	—	0.42 ± 0.05

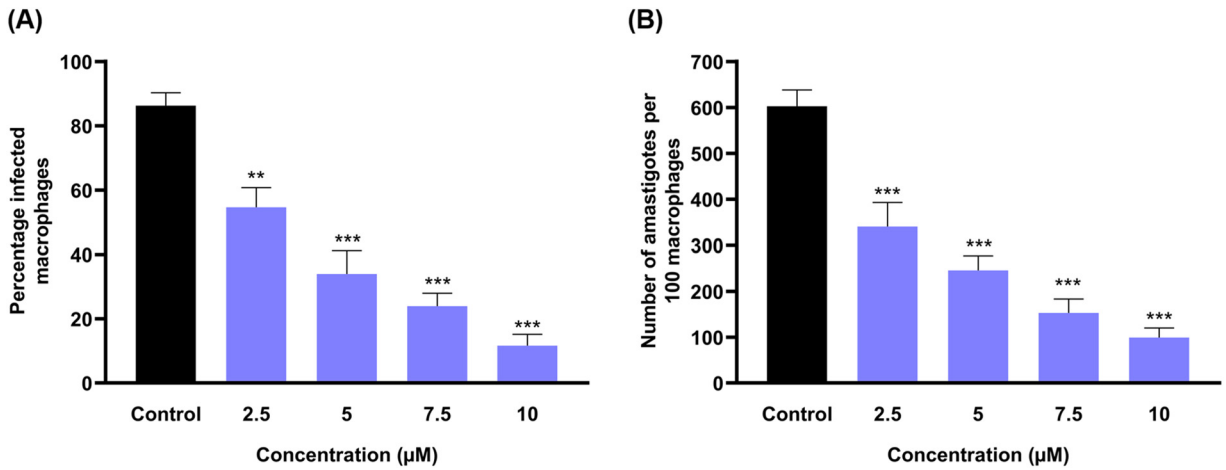

Fig. 2 Macrophage infection assay to determine the effect of the potent hit (**3m**) on intracellular amastigotes. (A) Percentage macrophage infection in the RAW 264.7 cell line after treatment with the potent hit (**3m**). (B) The number of amastigotes per 100 macrophages was determined by visual counting in treated and untreated cells. Results are expressed as the means ± standard deviation of three independent experiments. Significant differences were determined using Student's *t*-test (**$p < 0.01$ and ***$p < 0.001$) compared to control cells.

burden. In infected control cells, ~610 amastigotes were observed per 100 macrophages whereas only ~330, ~225, ~120, and ~75 amastigotes were observed per 100 macrophages after treatment with **3m** at 2.5 μM, 5 μM, 7.5 μM, and 10 μM, respectively (Fig. 2B). The reduction in intracellular parasitic load using **3m** at 2.5 μM, 5 μM, 7.5 μM, and 10 μM was ~46%, ~64%, ~83% and ~91%, respectively. Thus, the *ex vivo* assay confirms that treatment with **3m** significantly reduces the intracellular amastigote burden.

Furthermore, the specificity index (SPI) is calculated as the ratio of the promastigote IC_{50} value and amastigote IC_{50} value as mentioned previously.[20,21] This SPI value designates the probable targeted form of *Leishmania* preferred by **3m** as a killing strategy. A value below 0.4 refers to its action in promastigote form: an SPI above 2 mentions its priority towards the amastigote form, whereas a value between 0.4 to 2 reflects its activity in the direction of both the forms of the *Leishmania* parasite. The anti-amastigote IC_{50} value for **3m** is 2.63 ± 0.24 μM, as determined by a resazurin-based Alamar blue assay. **3m** exhibited an SPI value of 1.44, which reflects its specificity towards promastigote and amastigote forms of the parasites.

2.4 Cytotoxicity and selectivity index analysis

One of the essential aspects of evaluating the therapeutic potential of any bioactive molecule is to determine its toxicological profile. Thus, the cytotoxicity of **3m** was conducted in a panel of cell lines (J774A.1, N9, A549, and C2C12) at varied dosages (10 to 100 μM) using an MTT cell viability assay. The ability of NADPH-dependent cellular enzymes to reduce the MTT dye into purple-colored formazan crystals in the presence of viable cells constitutes a suitable parameter for toxicity assessment. **3m** displayed a dose-dependent change in cell viability across different cell lines. The comparative percentage viability in cell lines treated with **3m** was ~32%, ~46%, ~56%, ~73%, and ~93% at a dosage of 100, 75, 50, 25, and 10 μM, respectively. The CC_{50} values obtained for J774A.1, N9, A549, and C2C12 cell lines were 60.59 ± 3.28 μM, 54.64 ± 2.84 μM, 56.91 ± 2.66, and 71.80 ± 3.11, respectively using GraphPad™ Prism 8 (version 8.0.2) software. Furthermore, anti-amastigote activity was calculated to determine the selectivity index which is defined as a ratio of CC_{50} value to anti-promastigote. **3m** displayed a good selectivity index ranging from 8 to 11 across the tested cell lines. The CC_{50} values in various cell lines along with their selectivity index are illustrated in Table 2.

2.5 Plasmid relaxation assays

2.5.1 Simultaneous plasmid relaxation assay. Plasmid relaxation assays were performed to observe the effect of hit compounds (**3n** and **3m**) on *Ld*Top1LS activity under simultaneous conditions. The assay for topoisomerase I-mediated DNA relaxation demonstrated significant efficacy, ease of handling, and informative potential in the investigation of drug interactions with DNA. This methodology utilizes a supercoiled plasmid as a model to replicate the topological constraints inherent to genomic DNA, thereby providing a relevant platform for the study of drug binding dynamics. Camptothecin (CPT), a potent inhibitor of DNA topoisomerase I, triggers programmed cell death in amastigote and promastigote forms of *L. donovani* parasites. The cellular dysfunction induced by CPT in *L. donovani* promastigotes is marked by various cytoplasmic and nuclear characteristics typical of apoptosis. Additionally, CPT disrupts cellular respiration, leading to mitochondrial hyperpolarization facilitated by an oligomycin-sensitive $F_0 - F_1$ ATPase-like protein in leishmanial cells. In this assay, CPT is used as a positive control. In the simultaneous assay, substrate pHOT-1 DNA, *Ld*Top1LS enzyme, along with increasing concentrations of **3n** and **3m** were added to the reaction mixture. The experiment was performed under standard conditions with DNA and enzyme concentration at a molar ratio of 3 : 1 as mentioned in the 'Materials and methods' section (see ESI† file). There were four controls in the experiment, DNA (Fig. 3A, lane 1); DNA and enzyme (lane 2); DNA, enzyme, and DMSO (lane 3); and DNA, enzyme, and 60 μM CPT (lane 4). Then, **3n** and **3m** were added at concentrations of 50 μM, 100 μM, 200 μM, 400 μM, 800 μM, and 1600 μM (lanes 5–16). Both **3n** and **3m** inhibited the catalytic activity of *Ld*Top1LS at 800 μM and 1600 μM, respectively (Fig. 3A, lanes 9–10 and 15–16). **3n** resulted in almost 90% inhibition of the catalytic activity of *Ld*Top1LS at 1600 μM (lane 10). However, **3m** achieved 100% enzyme inhibition at 1600 μM (lane 16). Therefore, the inhibition of *Ld*TopILS activity by **3n** and **3m** occurred in a dose-dependent manner. **3m** was a more potent inhibitor of *Ld*Top1LS than **3n**, whose inhibitory action was comparable to CPT (Fig. 3A).

2.5.2 Pre-incubation plasmid relaxation assay. Pre-incubation relaxation assays were performed to investigate whether the inhibitor belongs to class I (topoisomerase poison) or a class II (catalytic inhibitor). The pre-incubation relaxation assay was performed in a similar manner to that of the simultaneous assay, except the enzyme was pre-incubated with **3n** and **3m** (50 μM, 100 μM, 200 μM, 400 μM, 800 μM, and 1600 μM separately) for 5 min at 37 °C followed by the addition of DNA (Fig. 3B, lanes 5–16). Pre-incubation at different concentrations of **3n** and **3m** followed by incubations with pHOT-1 DNA revealed significant inhibition at 200 μM (Fig. 3B, lanes 7 and 13, respectively). The complete inhibition of *Ld*Top1LS by **3n** and **3m** was observed at 800 μM (lanes 9 and 15). Therefore, **3n** and **3m** inhibit the free enzyme rather than the enzyme–substrate complex, suggesting that these compounds are class II (catalytic inhibitor) inhibitors of *Ld*Top1LS. The compounds exhibit cellular activity in the micromolar range (**3m** = 6.6 μM and **3n** = 24.5 μM); however, they only inhibit *Ld*Top1LS activity at 800 μM. Therefore, **3n** and **3m** possess antileishmanial activity through the inhibition of *Ld*Top1LS and *via* a cumulative effect on various other enzymes and mechanistic pathways that are crucial for the survival of *L. donovani.* Our laboratory is currently engaged in screening **3m** and **3n**

Table 2 Cytotoxicity analysis of potent hit (**3m**) in various cell lines and determination of selectivity index

Cell line	Percentage viability					CC_{50} (μM)	SI[a]	SI[b]
	100 μM	75 μM	50 μM	25 μM	10 μM			
J774A.1	34.11 ± 2.83	45.79 ± 3.08	55.66 ± 2.91	72.33 ± 3.13	96.32 ± 3.51	60.59 ± 3.28	9.18	23.03
N9	29.82 ± 2.37	44.67 ± 3.41	51.53 ± 3.52	70.88 ± 4.09	91.64 ± 3.67	54.64 ± 2.84	8.27	20.77
A549	27.08 ± 2.54	44.18 ± 3.64	55.22 ± 3.18	75.11 ± 3.88	92.74 ± 3.41	56.91 ± 2.66	8.62	21.63
C2C12	38.71 ± 2.98	49.79 ± 3.91	62.34 ± 2.86	74.91 ± 4.04	91.07 ± 3.15	71.80 ± 3.11	10.87	27.31

[a] SI: CC_{50} cell line/IC_{50} promastigote (6.6 ± 1.15 μM). [b] SI: CC_{50} cell line/IC_{50} amastigote (2.63 ± 0.24 μM).

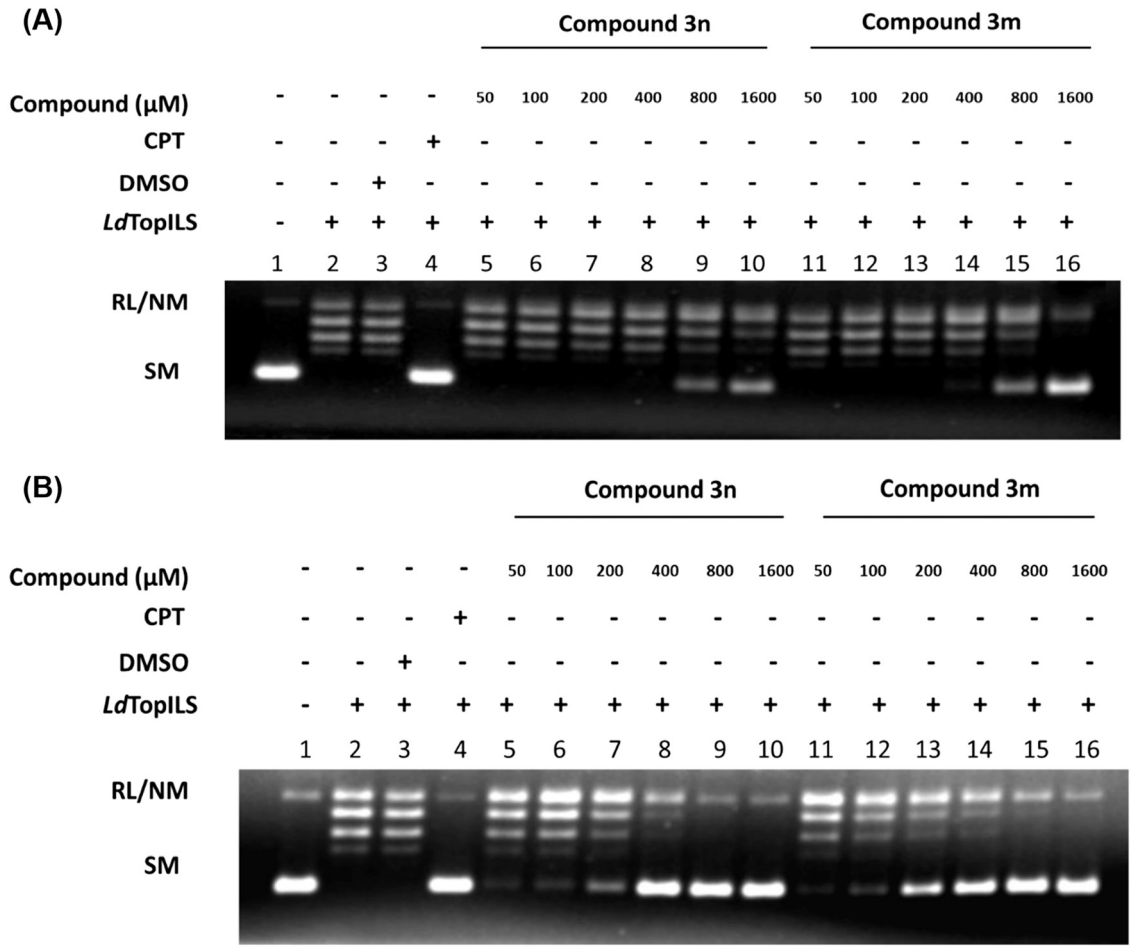

Fig. 3 Catalytic inhibition assay of *Ld*Top1LS enzyme by hit compounds (**3n** and **3m**). (A) Simultaneous plasmid relaxation assay: the inhibition of *Ld*Top1LS activity by synthesized hit compounds (**3n** and **3m**) was performed using agarose gel electrophoresis. The enzyme and pHOT-1 DNA substrate were mixed at a molar ratio of 3 : 1, along with camptothecin (CPT, 60 μM, positive control) or DMSO (4% v/v, vehicle control) or the potent hits. (B) Pre-incubation plasmid relaxation assay: this was performed similarly to simultaneous assay, except that the enzyme was pre-incubated with the hit compounds (**3n** and **3m**) separately for 5 min at 37 °C, followed by the addition of DNA. The first four lanes represent four controls in the experiment (lane 1: DNA, lane 2: DNA along with enzyme, lane 3: DNA, enzyme, and DMSO, and lane 4: camptothecin). Lanes 5 to 10 represent compound **3n** and lanes 11 to 16 represent compound **3m** at different concentrations ranging from 50 to 1600 μM. All samples were quantitated and visualized by EtBr (0.5 mg mL^{-1}) staining and a Gel Doc system (G-Box Chemi-XRQ-Genesys software). RL/NM: relaxed/nicked monomer; SM: supercoiled monomer.

against a range of kinases that play a crucial role in the lifecycle of *L. donovani*. This effort aims to evaluate their potential biological activities and contributions to our understanding of the disease.

2.6 Molecular docking analysis

Among the 44 synthesized compounds, **3m** showed the lowest IC_{50} value of 6.6 μM, followed by **3n** showing good leishmanicidal activity with an IC_{50} value of 24.56 μM. To learn more about their potential anti-leishmanial efficacies and further explore their binding affinities towards leishmanial protein targets, **3m** and **3n** were docked against leishmanial topoisomerase 1 (*Ld*Top1B) (PDB ID: 2B9S) (Fig. 4).[8] The binding energies of **3m** and **3n** against *Ld*Top1 were calculated as −7.7 Kcal mol^{-1} and −9.0 Kcal mol^{-1}, respectively, which is almost comparable to that of the binding energy of standard topoisomerase inhibitor (camptothecin): −9.8 kcal mol^{-1}. Further exploration of the protein–ligand interaction demonstrated that **3m** is involved in the formation of two hydrogen bonds with cytosine and thymine (DT-112 of E-chain) bases of the DNA portion of *Ld*Top1 (Fig. 4a and b). The trifluoromethyl group showcases distinct halogen bonds with adenine and thymine bases of the DNA fragment of the protein. Substantial van der Waals interactions were noted with DNA guanine and DNA adenine bases as well as Arg190 residue. Although **3n** showed lower binding energy, the protein–ligand interactions revealed one significant hydrogen bond formation between the hydrogen of 1*H*-indole with the Asn178 residue (Fig. 4c and d). Other non-significant π–σ and π–alkyl interactions were also encountered for **3n**. Camptothecin showed substantial hydrogen bonding interactions with the thymine base (DT-112 of the E-chain) of *Ld*Top1 similar to that of **3m**,

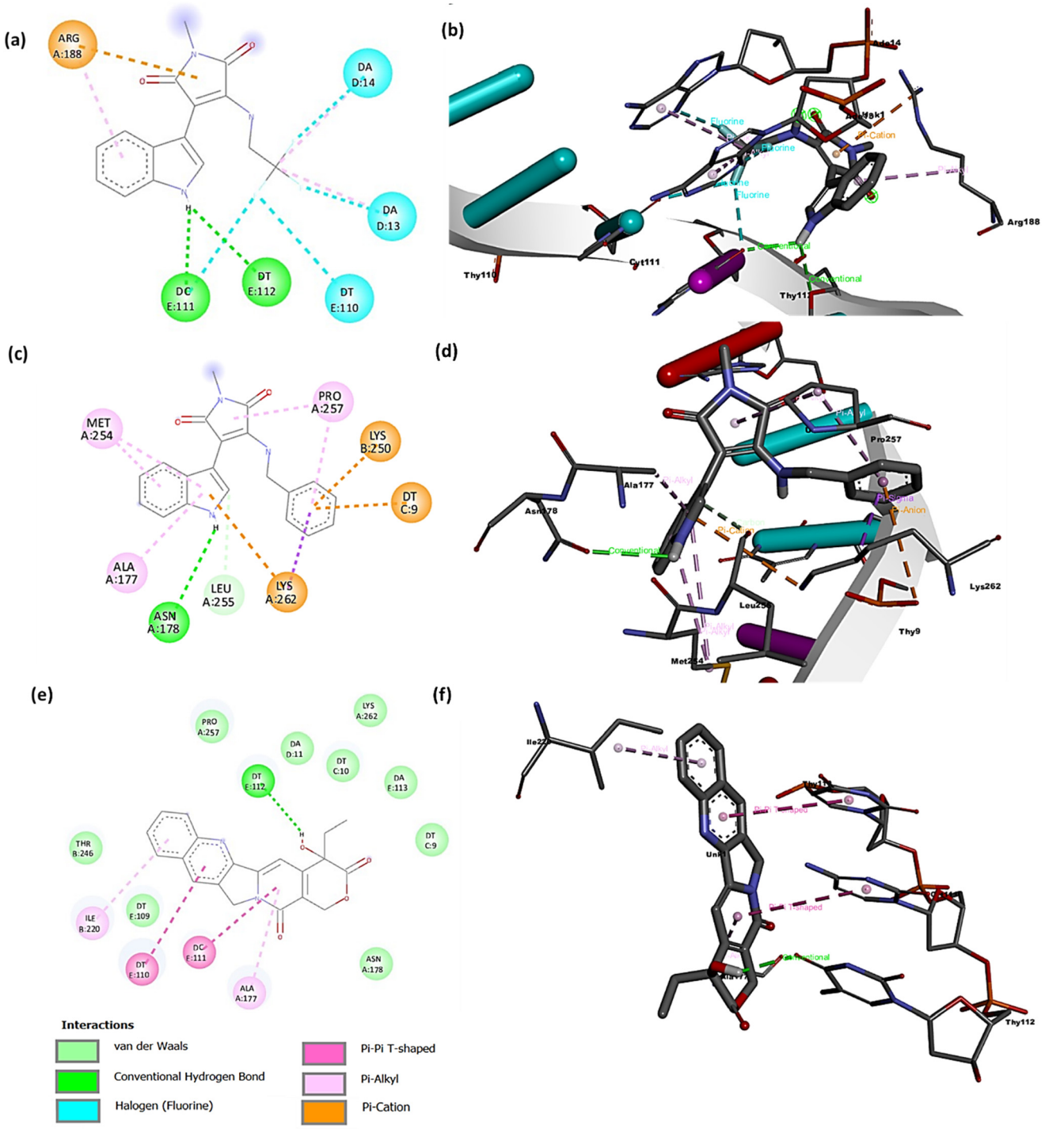

Fig. 4 Molecular docking analysis of compounds **3m** and **3n** against *Ld*Top1B (PDB ID: 2B9S) in comparison with the standard topoisomerase inhibitor, camptothecin. (a, c, and e) Represent 2D interactions, and (b, d, and f) represent 3D interaction images of compounds **3m**, **3n**, and camptothecin with their binding poses in the crystal structure of *Ld*Top1B.

explaining the efficient binding of **3m** to the active site of *Ld*Top1. Besides, camptothecin showed a number of van der Waals interactions with DNA adenine and DNA thymine bases, as well as Asn178, Thr246, Pro257, and Lys 262 residues in the active site of leishmanial topoisomerase1. Other non-significant π–π interactions were also noted (Fig. 4e and f). **3m** was also docked against human topoisomerase 1 (PDB ID: 1T8I) (Fig. 5a and b). The binding energies of **3m** against human topoisomerase I (topo1) were calculated to be −7.6 Kcal mol^{-1}. **3m** forms two hydrogen bonds with Tyr-426 and Met-428 residues in the A-chain of the protein, as well as a distinct halogen bond with the

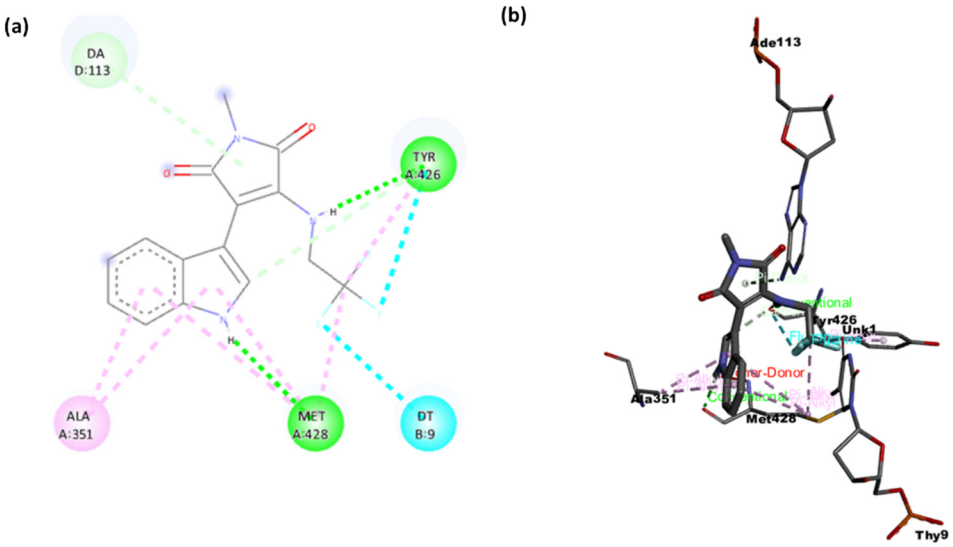

Fig. 5 Molecular docking analysis of compound **3m** against human topoisomerase 1; (a) represents 2D interactions and (b) represents 3D interaction images of compound **3m** with its binding pose in the crystal structure of the human topo1 enzyme (PDB ID: 1T8I).

thymine base (DT-9 of the B-chain) within the DNA fragment. The binding modes of **3m** in *Ld*Top1B and human topo1 are notably different in terms of their binding characteristics and interactions. Therefore, it is inappropriate to make a direct comparison between the two.

3. Conclusions

To accelerate the drug discovery process against leishmaniasis, we attempted to explore a new series of indole derivatives against the unique bi-subunit Top1B of the *Leishmania* parasite. We developed three series of hybrid indolylmaleimide molecules using nucleophilic substitution with aliphatic and heterocyclic amines as well as coupling with aromatic anilines and aminopyridines, together with aliphatic and aromatic amides *via* the Buchwald–Hartwig cross-coupling reaction. Preliminary screening revealed that one molecule (**3m**) possessed potent anti-leishmanial activity against *L. donovani* parasites among all the tested compounds. Various mechanistic studies and enzyme inhibition assays suggested that this indolylmaleimide derivative with a trifluoroethyl substitute is a potent inhibitor of leishmanial topoisomerase 1B, inhibiting the parasitic replication and transcription, ultimately leading to apoptotic cell death. Furthermore, *in silico* studies supported the experimental results by displaying significant protein–ligand interactions of **3m** with the target enzyme and confirming its strong binding affinity. Thus, the present study concluded that a fluorine atom in the alkyl chain was crucial for leishmanicidal activity. The potency of this compound could be due to the formation of a favorable halogen bond with the binding residues of the active site of the *L. donovani* topoisomerase 1B. This could be related to fluoro analogues strongly inhibiting the growth of the *Leishmania* parasite and could serve as potent anti-leishmanial scaffolds to further develop rational chemotherapeutic strategies against leishmaniasis.

Data availability

All the experimental and spectral data are available in the main article. The ^{1}H and ^{13}C NMR spectra of all the compounds are provided in the ESI.†

Author contributions

SD: synthesized and characterized the derivatives, performed molecular docking analysis, and wrote the original draft. RK: performed M.P. analysis of compounds. NK and SS: conducted and compiled the biological assays. PM and AR: performed and compiled the enzyme activity work. DKS: conceptualization, resources, review and editing, project administration, supervision. All authors have read and approved the final version of the manuscript.

Conflicts of interest

The authors confirm that this article has no conflict of interest.

Acknowledgements

Samarpita Das (SRF) is grateful to the Department of Science and Technology-Innovation in Science Pursuit for Inspired Research (DST-INSPIRE) for providing fellowship assistance (IF190906). We are grateful to the Indian Council of Medical Research (ICMR), Government of India, for supporting our work by awarding research grant to Dr. Deepak K. Sharma (Grant Number IIRP-2023-0227).

References

1 D. Steverding, The history of leishmaniasis, *Parasites Vectors*, 2017, **10**, 82, DOI: **10.1186/s13071-017-2028-5**.
2 T. Inceboz, Epidemiology and Ecology of Leishmaniasis, in *Current Topics in Neglected Tropical Diseases*, 2019, DOI: **10.5772/intechopen.86359**.
3 J. H. No, Visceral leishmaniasis: revisiting current treatments and approaches for future discoveries, *Acta Trop.*, 2016, **155**, 113–123, DOI: **10.1016/j.actatropica.2015.12.016**.
4 B. M. Roatt, J. M. d. O. Cardoso, R. C. F. De Brito, W. Coura-Vital, R. D. O. Aguiar-Soares and A. B. Reis, Recent advances and new strategies on leishmaniasis treatment, *Appl. Microbiol. Biotechnol.*, 2020, **104**, 8965–8977, DOI: **10.1016/j.ijid.2011.03.021**.
5 S. R. Uliana, C. T. Trinconi and A. C. Coelho, Chemotherapy of leishmaniasis: present challenges, *Parasitol*, 2017, **145**(4), 464–480, DOI: **10.1017/S0031182016002523**.
6 G. Mandal, V. Govindarajan, M. Sharma, H. Bhattacharjee and R. Mukhopadhyay, Drug Resistance in Leishmania, *Antimicrob. Drug Resist.*, 2017, 649–665, DOI: **10.1007/978-3-319-46718-4_42**.
7 P. Kour, P. Saha, S. Bhattacharya, D. Kumari, A. Debnath, A. Roy, D. K. Sharma, D. Mukherjee and K. Singh, Design, Synthesis, and biological evaluation of 3, 3′-diindolylmethane N-linked glycoconjugate as Leishmanial Topoisomerase IB inhibitor with reduced cytotoxicity, *RSC Med. Chem.*, 2023, **14**(10), 2100–2114, DOI: **10.1039/D3MD00214D**.
8 P. Kour, P. Saha, D. K. Sharma and K. Singh, DNA topoisomerases as a drug target in Leishmaniasis: Structural and mechanistic insights, *Int. J. Biol. Macromol.*, 2024, **256**, 128401, DOI: **10.1016/j.ijbiomac.2023.128401**.
9 L. N. Cooney, K. D. O'Shea, H. J. Winfield, M. M. Cahill, L. T. Pierce and F. O. McCarthy, Bisindolyl Maleimides and Indolylmaleimide Derivatives—A Review of Their Synthesis and Bioactivity, *Pharmaceuticals*, 2023, **16**(9), 1191–1215, DOI: **10.3390/ph16091191**.
10 A.-C. Schmöle, A. Brennführer, G. Karapetyan, R. Jaster, A. Pews-Davtyan, R. Hübner, S. Ortinau, M. Beller, A. Rolfs and M. J. Frech, Novel indolylmaleimide acts as GSK-3β inhibitor in human neural progenitor cells, *Bioorg. Med. Chem.*, 2010, **18**(18), 6785–6795, DOI: **10.1016/j.bmc.2010.07.045**.
11 P. Lassota, G. Singh and R. Kramer, Mechanism of topoisomerase II inhibition by staurosporine and other protein kinase inhibitors, *J. Biol. Chem.*, 1996, **271**(42), 26418–26423, DOI: **10.1074/jbc.271.42.26418**.
12 P. M. de Iturrate, V. Sebastián-Pérez, M. Nácher-Vázquez, C. S. Tremper, D. Smirlis, J. Martín, A. Martínez, N. E. Campillo, L. Rivas and C. Gil, Towards discovery of new leishmanicidal scaffolds able to inhibit Leishmania GSK-3, *J. Enzyme Inhib. Med. Chem.*, 2020, **35**(1), 199–210, DOI: **10.1080/14756366.2019.1693704**.
13 D. K. Sharma, V. S. Rajput, S. Singh, R. Sharma, I. A. Khan and D. Mukherjee, *ChemistrySelect*, 2016, **1**(9), 1954–1958, DOI: **10.1002/slct.201600253**.
14 S. Das, K. K. Verma, H. K. Indurthi, P. Saha and D. K. Sharma, Efficient Pd-catalysed Synthesis of 3-Amino-4-indolylmaleimides and 3-Amido-4-indolylmaleimides, *ChemistrySelect*, 2024, **9**(1), e202304745, DOI: **10.1002/slct.202304745**.
15 S. Das, P. Goswami, V. K. Verma, H. K. Indurthi, M. Kumar, B. Koch and D. K. Sharma, Rapid access to 7-substituted cycloalkylamino and alkylamino analogues of 4-methylcoumarin reveals surprising emitters, *Dyes Pigm.*, 2023, **217**, 111407–111415, DOI: **10.1016/j.dyepig.2023.111407**.
16 J. Singh, M. I. Khan, S. P. S. Yadav, A. Srivastava, K. K. Sinha, P. Das and B. Kundu, L-Asparaginase of Leishmania donovani: Metabolic target and its role in Amphotericin B resistance, *Int. J. Parasitol.:Drugs Drug Resist.*, 2017, **7**(3), 337–349, DOI: **10.1016/j.ijpddr.2017.09.003**.
17 E. van den Bogaart, G. J. Schoone, P. England, D. Faber, K. M. Orrling, J.-C. Dujardin, S. Sundar, H. D. Schallig and E. R. Adams, Simple colorimetric trypanothione reductase-based assay for high-throughput screening of drugs against Leishmania intracellular amastigotes, *Antimicrob. Agents Chemother.*, 2014, **58**(1), 527–535, DOI: **10.1128/AAC.00751-13**.
18 F. Conceicao-Silva and F. N. Morgado, Leishmania spp-host interaction: there is always an onset, but is there an end?, *Front. Cell. Infect. Microbiol.*, 2019, **9**, 330–343, DOI: **10.3389/fcimb.2019.00330**.
19 T. Van Assche, M. Deschacht, R. A. I. da Luz, L. Maes and P. Cos, Leishmania–macrophage interactions: Insights into the redox biology, *Free Radical Biol. Med.*, 2011, **51**(2), 337–351, DOI: **10.1016/j.freeradbiomed.2011.05.011**.
20 G. D. Badenhorst, C. Kannigadu, J. Aucamp and D. D. David, Probing O-substituted nifuroxazide analogues against Leishmania: Synthesis, in vitro efficacy, and hit/lead identification, *Eur. J. Pharm. Sci.*, 2022, **176**, 106242–106252, DOI: **10.1016/j.ejps.2022.106242**.
21 N. H. Zuma, J. Aucamp, H. D. J. van Rensburg and D. D. N'Da, Synthesis and in vitro antileishmanial activity of alkylene-linked nitrofurantoin-triazole hybrids, *Eur. J. Med. Chem.*, 2023, **246**, 115012–115020, DOI: **10.1016/j.ejmech.2022.115012**.

